Design Of All-Normal Dispersion With Ge11.5As24Se64.5/Ge20Sb15Se65 Chalcogenide PCF Pumped At 1300nm For Supercontinuum Generation

Alireza Cheshmberah
Shahid Rajaee Teacher Training University
Mahmood Seifouri
Shahid Rajaee Teacher Training University
Saeed Olyaee (s_olyaee@srttu.edu)
Shahid Rajaee Teacher Training University https://orcid.org/0000-0002-6154-7646

Research Article

Keywords: Supercontinuum, dispersion, photonic crystal fiber, chalcogenide, nonlinear

Posted Date: June 25th, 2021

DOI: https://doi.org/10.21203/rs.3.rs-620957/v1

Version of Record: A version of this preprint was published at Optical and Quantum Electronics on August 6th, 2021. See the published version at https://doi.org/10.1007/s11082-021-03099-0.

Design of all-normal dispersion with $Ge_{11.5}As_{24}Se_{64.5}/Ge_{20}Sb_{15}Se_{65}$ chalcogenide PCF pumped at 1300nm for Supercontinuum generation

Alireza Cheshmberah[1], Mahmood Seifouri[2], and Saeed Olyaee[1,*]

[1] Nano-photonics and Optoelectronics Research Laboratory (NORLab), Shahid Rajaee Teacher Training University, 16788-15811, Tehran, Iran

[2] Photonic Devices Research Lab, Shahid Rajaee Teacher Training University, Tehran, Iran

*Corresponding Author: s_olyaee@sru.ac.ir

Abstract: Supercontinuum spectrum generation is a process in which laser beam in femtoseconds and high power (kilowatts) is converted into a broad-spectrum beam of light after passing through a specific environment. Of course, achieving this range comes with many limitations. In this paper, photonic crystal fibers are used as a substrate for input pulse due to the ability to control dispersion and loss, and creating single-mode operating conditions. One of the main factors for the formation of supercontinuum spectra of injection pulses is maintaining the nonlinear performance of this type of fiber by controlling the effective mode area and also using chalcogenides (nonlinear coefficients about 100 times higher than silica) in their structure. In the proposed structure, a photonic crystal fiber with silica base element and air cavities with hexagonal structure with the center of $Ge_{11.5}As_{24}Se_{64.5}$ chalcogenide element have been used to provide the nonlinear property of the structure. Also, in this structure, a ring of $Ge_{20}Sb_{15}Se_{65}$ chalcogenide elements has been used to reduce the effective mode region and create a flat dispersion curve at a wavelength of 1300 nm (second telecommunication window). The input pulse power is 10 kW and its width is 50 femtoseconds, which has caused the range of the supercontinuum from 800 nm to 1900 nm. This structure can be used to provide the required wavelengths as a carrier in a wavelength division multiplexing (WDM).

Keywords: Supercontinuum; dispersion; photonic crystal fiber; chalcogenide; nonlinear.

1. Introduction

In recent years, photonic crystals or dielectric structures whose refractive index changes periodically have come to the attention of researchers. The behavior of these crystals against the propagation of waves is similar to the behavior of semiconductor crystals against the emission of electrons. In fact, this is due to the similarity of the Schrodinger equation in solid state physics and the Helmholtz equation in electromagnetism. The refractive index behavior in the Helmholtz equation is the same as the potential electric behavior in the Schrodinger equation. Therefore, the behavior of photonic crystals (structures with alternating refractive index) against photons is similar to the behavior of semiconductor crystals (structures with alternating electric potential) against electrons. To emit an electromagnetic wave, there must be a match between the emitted wavelength and the dimensions of the photonic crystal. Millimeter-sized photonic crystals can be designed to control microwaves, and micrometer-sized crystals can be designed to control infrared waves. The propagation of waves in an environment is described by the dispersion relationship between the frequency and the wave vector. The dispersion relationship can be quite complex considering a heterogeneous substance. The propagation of waves in a crystal will depend on how the wave enters the crystal, in other words, the wave propagation must be considered. The periodicity of the photonic crystal structure is the main reason for the formation

of the band structure. The wavelengths of light that are allowed to propagate are called modes. Permitted diffuse modes form energy bands. In the frequency domain, within the band structure, there are continuous and boundary frequency ranges that do not allow the propagation of waves in the photonic crystal in these areas (Saldaña-Díaz et al. 2019; Mohebzadeh-Bahabady and Olyaee 2020; Guo et al. 2021; Prandin 2021; Arman and Olyaee 2020; Ferhat et al. 2018; Russell 2003; Veisi et al. 2021).

Photonic crystal fibers (PCFs) are novel light waveguide structures that have drawn researchers' interest in recent years. More recently, fibers have been suggested by researchers for various applications, including sensor design, optical telecommunication systems, due to their specific advantages and features. The focal points of these filaments incorporate the simplicity of dispersion designing and the control of nonlinear parameters over the required wavelength run. One of the applications of these strands is to deliver a supercontinuum (SC) spectrum. The supercontinuum range may be a broadband coherent range that will be created by infusing a high power and femto second input pulse to a nonlinear environment (Yan et al. 2013; Chauhan et al. 2020; Dashtban et al. 2021; Hui et al. 2013).

Creating a supercontinuum range based on photonic crystal fiber requires fitting of dispersion profile and improving of nonlinear parameters. Dispersion in a fiber occurs when an optical pulse travels through an optical fiber and its power is dispersed over time, so the pulse propagates over a wider period of time. The main kinds of dispersion are modal, material, waveguide, polarization, and nonlinearity. Dispersion can occur in two normal and anomalous areas. In a normal area, the group velocity is less than the phase velocity, in which the refractive index increases with increasing frequency (Medjouri and Abed 2019b).

In an environment with anomalous dispersion, unlike a normal environment, the phase velocity is higher than the group velocity, and also in this environment, a fuzzy velocity greater than the speed of light in a vacuum can be achieved. In this area, the dispersion plot no longer works as expected and we see strong absorption.

In the area of anomalous dispersion, soliton dynamics, dispersive wave generation, the change in self-Raman frequency is decisive in the process of SC production, but in the region of normal dispersion, self-phase modulation (SPM) and optical wave breaking (OWB) are effective in supercontinuum production (Wang et al. 2018).

In 2015, Saini *et al*. designed a triangular-core photonic crystal fiber with As_2Se_3 and supercontinuum produced (1.9 –10 μm) with pump pulse at 4.5 μm and average power of 0.75 kw (Saini et al. 2015). Also, a design in Chg As_2Se_3 PCFs, by input pulse at 2.5 μm which can increase the SC spectrum more than 4 μm (Hu et al. 2010) was proposed. Sharma *et al*. have obtained broadband SCG with bandwidth of 6.3 μm by utilizing dispersion engineered $GeSe_2$-As_2Se_3-PbSe based chalcogenide (Chg) PCF (Sharma et al. 2020). In addition, mid-IR supercontinuum in wavelength range of 8 μm in an As_2Se_3 PCF with power of 10 kW was reproduced (Yuan 2013). In 2019, a supercontinuum from 2.43 μm to 4.85 μm was achieved by pumping into a Chg glass optical fiber $As_{39}Se_{61}$ with wavelengths 3.45 μm (Medjouri and Abed 2019a). In 2018, a spectra spanning from 480 nm to over 2000 nm with 215 W of average power was achieved (Zhao et al. 2018).

All normal dispersion and nonlinear Chg glass were recently studied (Medjouri et al. 2019). Seven rings of air holes arranged in a hexagonal lattice surround the $Ga_8Sb_{32}S_{60}$. Simulations showed that the wavelength range from 1.65 μm to 9.24 μm at 20 dB in this structure was broadband and completely (Medjouri et al. 2019). For more, a type of Chg AsSe2 for broadband MIR light source was designed. Broadband coherent SC generation with more than 3 octave spanning from 1.7 to 14 μm achieved (Diouf et al. 2016).

Recently, we presented a paper on the use of a 5 mm photonic crystal fiber based on chalcogenide elements, with a pulse input of 100 fs and a power of 1 kW of spectral bandwidth of 5 μm produced in the third telecommunication window (1550 nm), which used in WDM as a carrier in optical telecommunications (Cheshmberah et al. 2020).

In this paper, the dispersion engineered Chg PCF is analyzed, which can be used in ANDi areas to produce flat broadband supercontinuum spectra. Bandwidth of 1100 nm with pump power equal to 10 kW is given by the hexagonal chalcogenide PCF made from $Ge_{11.5}As_{24}Se_{64.5}/Ge_{20}Sb_{15}Se_{65}$ pumped at 1300 nm. In addition, the zero-dispersion wavelength (ZDW) at the second telecommunication is achieved. Although the spectral bandwidth of the SC in this paper is shorter than the previous paper, it also has a shorter length (1 mm), which is an advantage of this designed PCF. The SC in the previous article (Cheshmberah et al. 2020) is in the third telecommunication window (1550 nm), but here the central wavelength of the SC is 1300 nm, which changes its use in WDM.

2. The principles

The supercontinuum generation's mathematical modeling is based on a generalized time-domain nonlinear Schrödinger equation (GNLSE), which takes the linear and nonlinear effects into account, for a pulse envelope that varies slowly A (z, t) (Siwach et al. 2018):

$$\frac{\partial A(z,t)}{\partial z}+\frac{\alpha}{2}A(z,t)-\sum_{n>=0}^{n}\beta_n\frac{i^{n+1}}{n!}\frac{\partial^n A(z,t)}{\partial t^n}= \tag{1}$$

$$i(\gamma+i\frac{\alpha_2}{2A_{eff}})\times(1+i\tau_{shock}\frac{\partial}{\partial t})[A(z,t)\int_0^{+\infty}R(t')\left|A(z,t-t')\right|^2dt']$$

where, α is the loss coefficient and $\beta_n(\omega_0) = d^n\beta/d\omega^n$ is the dispersion coefficient of n-th order associated with the propagation constant $\beta(\omega_0)$ extension of the Taylor series around a pump frequency ω_0. The first term β_0 provides an efficient propagating optical mode index and the second and third terms (β_1 and β_2) are related to the group velocity and the GVD of the pulse (Chauhan et al. 2018; Hui et al. 2015).

The response function, including the Raman and Kerr nonlinearities, is represented by:

$$R(t') = (1-f_R)\delta(t'-t_e) + f_R h_R(t') \tag{3}$$

where, (τ_1) and (τ_2) are Raman duration and lifetime, f_R and $h_R(t')$ are respectively fractional contribution of the Raman response and Raman response function (Vyas et al. 2016):

$$h_R(t') = \frac{\tau_1^2+\tau_2^2}{\tau_1}\exp(-\frac{t'}{\tau_2})\,\mathrm{Sin}(-\frac{t'}{\tau_1}) \tag{4}$$

where, f_R is equal to 0.031 for $Ge_{11.5}As_{24}Se_{64.5}$ chalcogenide glass, and $\tau_1 = 15.5$ fs and $\tau_2 = 230.5$ fs are two adjustable parameters.

The ultra-short pulse of light which can be produced by mode-locking fiber lasers (Hui et al. 2019; Hui et al. 2020; Shi et al. 2014), due to the optical effect of the environment, alters the refractive index by introducing it into the environment. By producing a fuzzy shift in the pulse, these differences in the refractive index contribute to shifts in the frequency spectrum. As the field increases, there will also be major changes in the nonlinear coefficient, allowing the phase to change; the angular frequency will adjust as a result (Diouf et al. 2017).

$$\varphi=\tilde{n}k_0L = (n+n_2|E|^2)k_0L \tag{8}$$

$$\omega(t)=\frac{-d\varphi_{NL}(t)}{dt} = -n_2kL\frac{dI(t)}{dt} \tag{9}$$

Using the Sellmeier dispersive model, the refractive index depending on the wavelength of $Ge_{11.5}As_{24}Se_{64.5}$ can be obtained as:

$$n^2(\lambda) = 1+\frac{5.78525\lambda^2}{\lambda^2-0.28795^2}+\frac{0.39705\lambda^2}{\lambda^2-30.39388^2} \tag{10}$$

3. Results and discussions

The proposed structure is shown in Fig. 1, which is made of silica and hexagonal lattice of air-holes and the inner ring of Chg $Ge_{20}Sb_{15}Se_{65}$ centered on $Ge_{11.5}As_{24}Se_{64.5}$ .Dc is the core radius and equal to 0.284 and D2 is made of $Ge_{20}Sb_{15}Se_{65}$ equal to 0.36 µm. Both of (Λ1) and (Λ2) are 1 µm.

The difference in refractive index between the central element of the photonic crystal fiber structure, chalcogenide, and silica causes the beam to concentrate in the center of the structure due to the total internal reflection (TIR). For this reason, $Ge_{11.5}As_{24}Se_{64.5}$ has been used here.

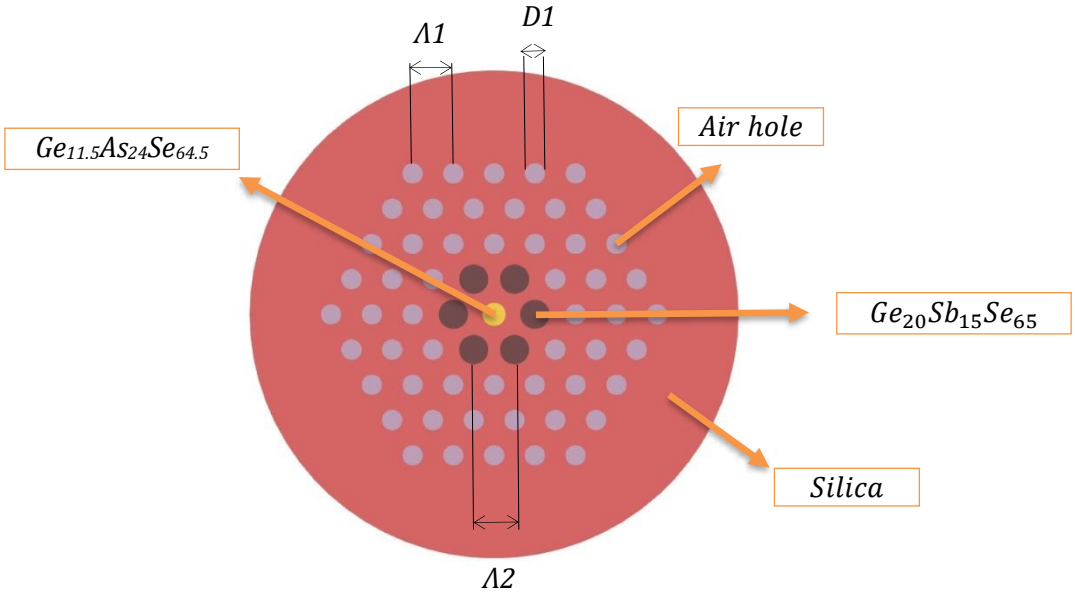

Figure 1. The cross section of proposed PCF.

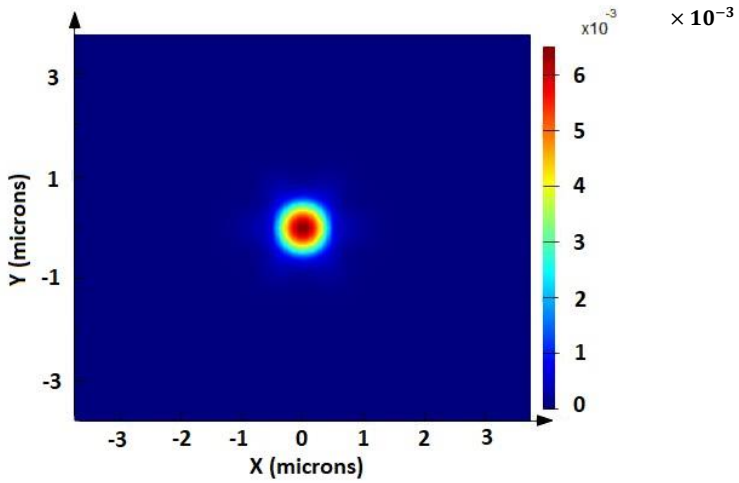

Figure 2. The distribution of the propagating mode's electric field.

In the continuation of the dispersion analysis, the effective refractive index (n_{eff}) of the basic mode of the photonic crystal fiber was first measured and changes in operating wavelength (λ) were shown in Figure 3. We have found that the magnitude of effective mode region of the propagating mode is less sensitive to the structural parameters after investigating the impact of small variations in the values of d2. The closer the refractive index changes to the fiber core

refractive index, the better the fiber achieves. As shown in the figure, we will have the least changes in refractive index at wavelengths of 1 μm to 1.7 μm.

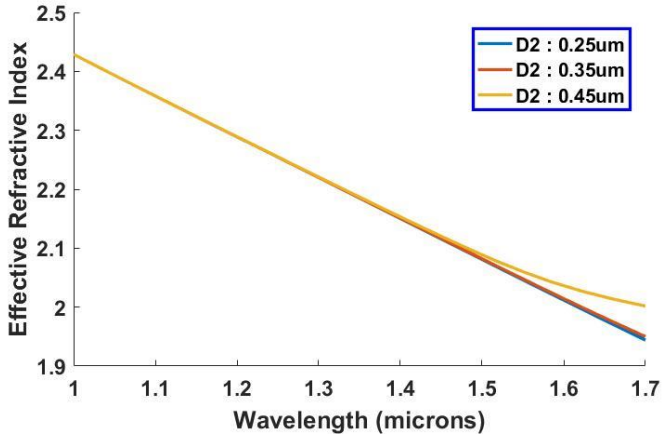

Figure 3. Changing n_{eff} of the main mode with respect to the wavelengths for different D2 values.

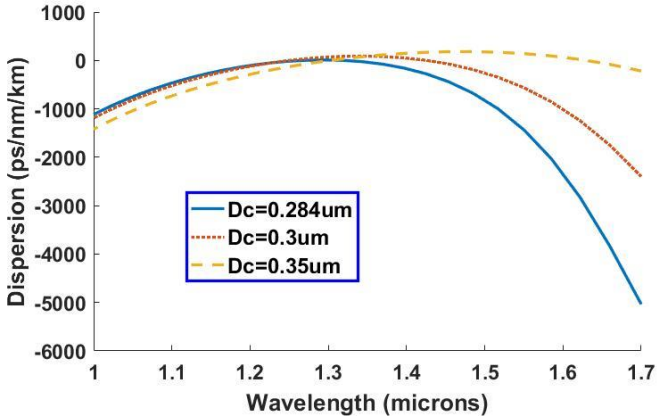

Figure 4. The effect on the dispersion profile of core radius changes.

The dispersion of the group velocity is a wavelength feature, and the dispersion profile is engineered by the variation of the hole radius and the constant of the lattice. The dispersion profile is calculated for various core and pitch sizes in order to achieve the optimum structure. For various core sizes, Fig. 4 shows the dispersion profile. If the core radius is 0.284 μm, the dispersion is very poor at 1300 nm in the ANDi region and the profile is smooth. Decrease in the core radius does not dramatically affect the overall dispersion value, but the wavelength appears to be smaller and the dispersion profile still remains in the area of anomalous dispersion (Zhang et al. 2018).

In order to produce a flat dispersion profile, a Chg ring added around the core. The dispersion anomaly increases without this ring of chalcogenide holes and the dispersion profile is not flat. As shown in the Figure. 5 when D2 is greater than 0.32 μm, the dispersion slope changes from the anomalous dispersion region to the ANDi and the dispersion curve peak arrives at shorter wavelengths (Kalantari et al. 2018; Karim et al. 2017).

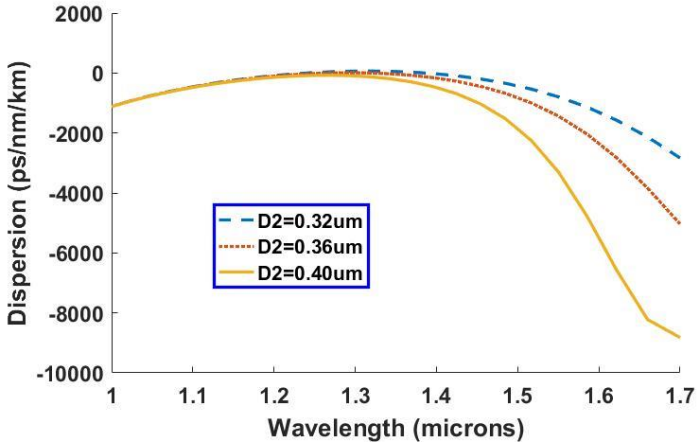

Figure 5. The impact of the internal ring radius of the Chg.

Another factor affecting dispersion is the number and radius of cladding air holes, but it has little influence on dispersion, since due to the core and the Chg ring, the main mode is concentrated in the middle. Moreover, we should not eliminate them due to the ineffectiveness of the air cavities, because in fact, the beam leaves the center and deviates towards the air cavities, so that they can not be removed from the structure (Figure 6).

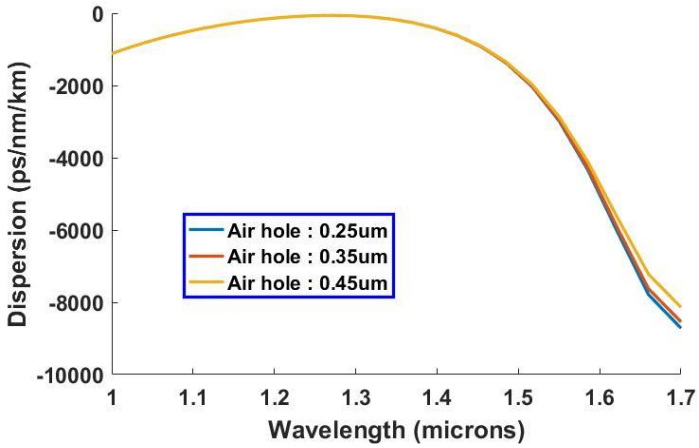

Figure 6. The effect of the radius of the cladding air holes on dispersion.

The presence or absence of chalcogenide holes is shown in Fig. 7. Obviously, we need a flat dispersion profile at that range of wavelengths to provide a symmetrical supercontinuum spectrum around 1300 nm wavelengths. When air holes are used instead of Chg in the inner ring of the proposed structure, ZDW occurs at lower wavelengths and enters the anomalous dispersion region at higher wavelengths, which is undesirable for symmetrical supercontinuum spectra to be generated.

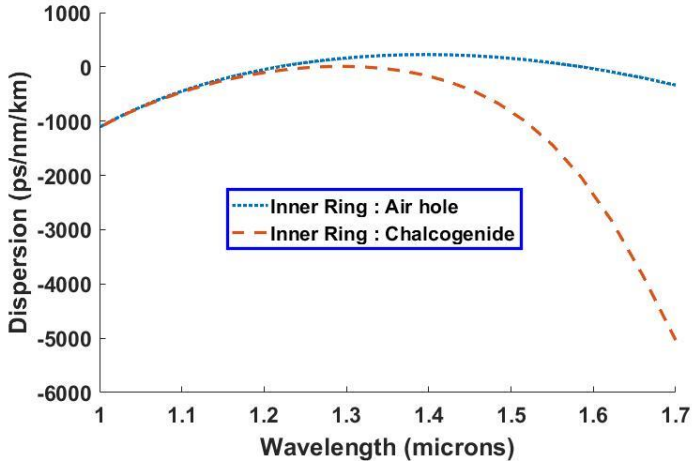

Figure 7. The impact on the dispersion of the inner ring material.

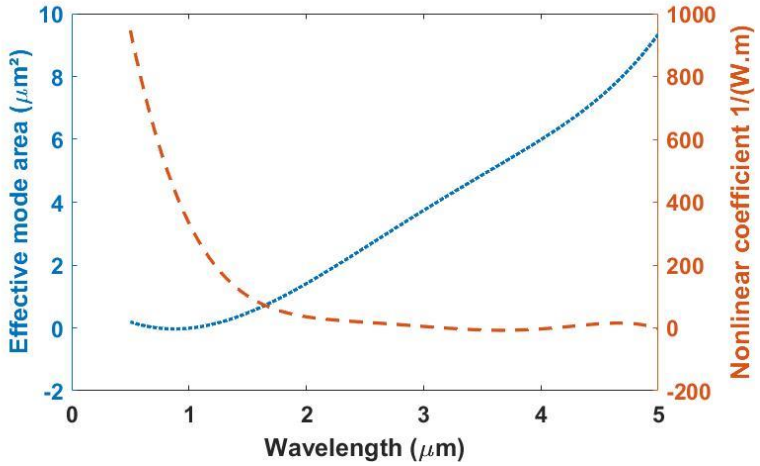

Figure 8. The effective mode area and the nonlinear coefficient (Dc=0.284 μm, D2 = 0.36 and Λ2=1 μm).

The effective mode area of the designed PCF is shown in Fig 8. We found that at short wavelength, the proposed PCF showed a small effective mode area. At a pump wavelength of approximately 1300 nm, A_{eff} was about 0.2 μm^2. Also We find that $Ge_{11.5}As_{24}Se_{64.5}$ PCF has a high nonlinear coefficient (γ= 232).

Simulation results show that we achieve spectral enlargement from 900 nm to 1800 nm by using 50 fs pulse length and peak power of 1000 W (Figure 9a). The spectral broadening is mainly around 700 nm, from 900 nm to 1600 nm, by using 150 fs pulse length (Figure 9c).

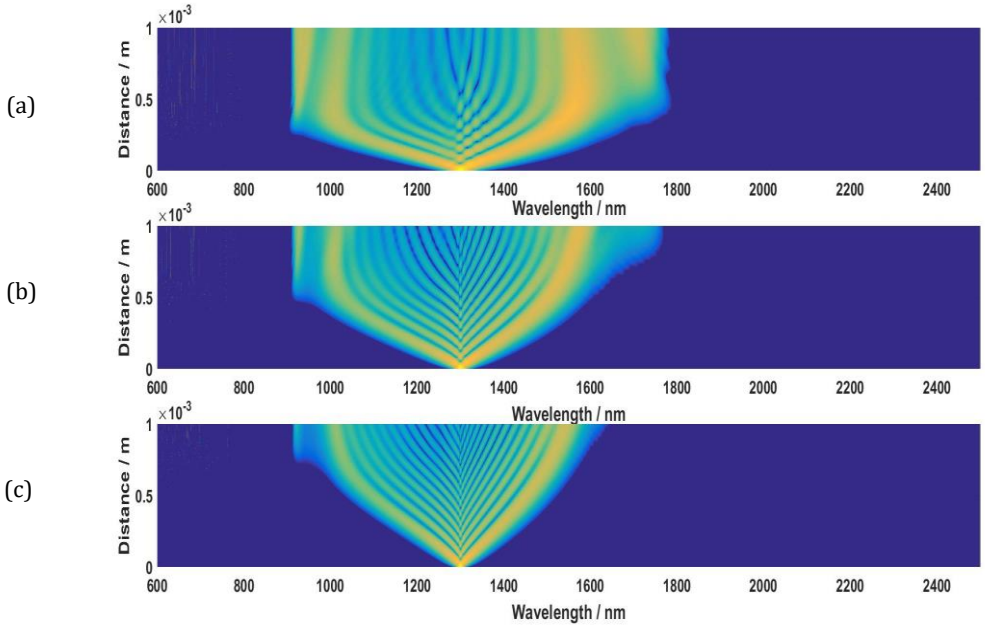

Figure 9. SC generation for pulse durations of 50, 100, and 150 fs and pump wavelength 1300 nm, peak power of 1000 W.

It is not suitable for the development of SC, according to the drawn diagrams, to increase the radius of the inner chalcogenide holes and also to reduce the distance between them due to the presence of the dispersion profile in the normal dispersion field.

The SC range obtained at pumped wavelength is compared with references (Li et al. 2019; Romano et al. 2020; Maji and Chaudhuri 2014; Xing et al. 2018; Maji et al. 2015) in Table 2. Proposed Chg core PCF has a short duration with a wide bandwidth than those recently released, and can be selected from the table. In addition, the proposed $Ge_{11.5}As_{24}Se_{64.5}$ PCF indicates a high potential for broadband and ultra-flat SC spectrum generation that ranges from 800 nm to 1900 nm, which is useful for WDM in 1300 nm.

The pulse evolution and spectral expansion at 1 mm of the proposed PCF duration is shown in Figure 10. In this case, in the simple quasi-TE mode, the period of the input pulse is 50 fs, where its power is 10 kW at a middle wavelength of 1300 nm. It is shown that, after approximately 0.3 mm, the spectrum reaches relative equilibrium and is stable at 0.3 mm (Seifouri et al. 2017a; Krishna et al. 2017; Seifouri et al. 2017b).

Table 2. SC generated spectra confronted to PCF designs made of various types of ChG glass.

Reference	ChG glass	Pumping wavelength (μm)	SC bandwidth (nm)
Li et al. 2019	As_2Se_3	4.3	1030
Romano et al. 2020	Thulium-doped	1.9	700
Maji and Chaudhuri 2014	Water or ethanol	1.8	450
Xing et al. 2018	GeAsSe - AsSe	2.08	420
Maji et al. 2015	As_2S_3	2.8	700
This work	$Ge_{11.5}As_{24}Se_{64.5}$/ $Ge_{20}Sb_{15}Se_{65}$	1.3	1100

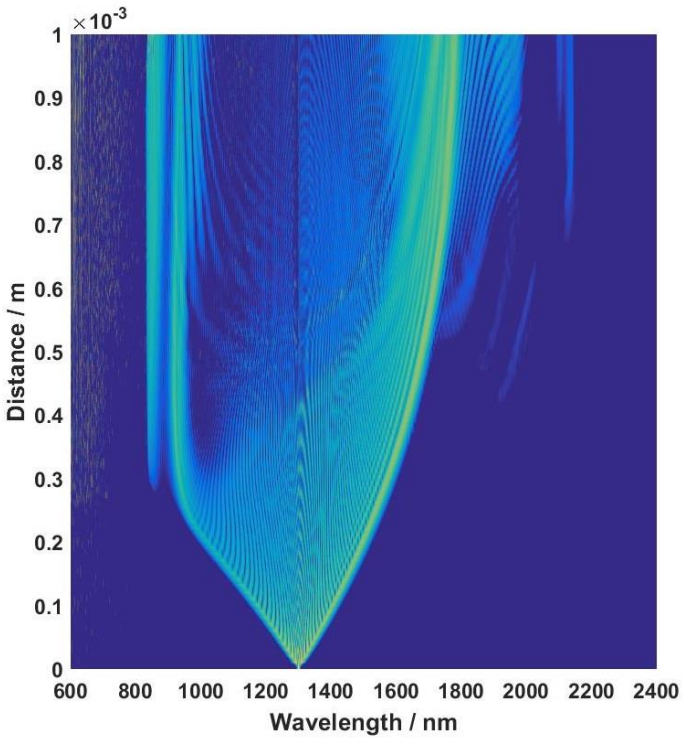

Figure 10. The spectral evolution of the generation of SC by pumping in a 1 mm length of the proposed structure 50 fs pulse period and 10 kW peak power.

4. Conclusion

In summary, for coherent broadband and ultraflat-top SC generation, we have studied an all-normal dispersion and highly nonlinear PCF dependent chalcogenide. The proposed PCF consists of a core made of $Ge_{11.5}As_{24}Se_{64.5}$ surrounded by rings of $Ge_{20}Sb_{15}Se_{65}$ and air holes. By changing structural parameters, the PCF was designed for pumping at wavelengths of 1300nm. The presented design allowed the supercontinuum bandwidth of 1100 nm at power of 10 kW to be obtained. The generated SC with a central wavelength of 1300 nm can be used in WDM as a carrier.

Acknowledgements

This research has been done in Nano-photonics and Optoelectronics Research Laboratory (NORLab) and the authors would like to thank Shahid Rajaee Teacher Training University for supporting of this research project.

Funding

This work was supported by Shahid Rajaee Teacher Training University (SRTTU).

Conflicts of interest

The authors declare no conflict of interest.

References

Arman H., Olyaee, S.: Improving the sensitivity of the HC-PBF based gas sensor by optimization of core size and mode interference suppression. Opt. Quant. Electron. **52**, 1-10 (2020).

Chauhan, P., Kumar, A., Kalra, Y.: Mid-infrared broadband supercontinuum generation in a highly nonlinear rectangular core chalcogenide photonic crystal fiber. Optical Fiber Technol. **46**, 174-178 (2018).

Chauhan, P., Kumar, A., Kalra, Y.: Numerical exploration of coherent supercontinuum generation in multicomponent $GeSe_2$-As_2Se_3-PbSe chalcogenide based photonic crystal fiber. Optical Fiber Technol. **54**, 102100 (2020).

Cheshmberah, A., Seifouri, M., Olyaee, S.: Supercontinuum generation in PCF with As_2S_3/$Ge_{20}Sb_{15}Se_{65}$ Chalcogenide core pumped at third telecommunication wavelengths for WDM. Opt. Quantum Electron. **52**, 1-14 (2020).

Dashtban, Z., Salehi, M. R., Abiri, E.: Supercontinuum generation in near- and mid-infrared spectral region using highly nonlinear silicon-core photonic crystal fiber for sensing applications. Photon. Nanostructures – Fundamental and Applications 46, 100942 (2021).

Diouf, M., Salem, A. B., Cherif, R., Saghaei, H., Wague, A.: Super-flat coherent supercontinuum source in $As_{38.8}Se_{61.2}$ chalcogenide photonic crystal fiber with all-normal dispersion engineering at a very low input energy. Appl. Opt. **56**, 163-169 (2017).

Diouf, M., Salem, A. B., Cherif, R., Wague, A., Zghal, M.: High power broadband mid-infrared supercontinuum fiber laser using a novel chalcogenide $AsSe_2$ photonic crystal fiber. Optical Materials **55**, 10-16 (2016).

Ferhat, M. L., Cherbi, L., Haddouche, I.: Supercontinuum generation in silica photonic crystal fiber at 1.3 μm and 1.65 μm wavelengths for optical coherence tomography. Optik **152**, 106-115 (2018).

Guo, Y., Yuan, J., Wang, K., Wang, H., Cheng, Y., Zhou, X., Yan, B., Sang, X., Yu. C.: Generation of supercontinuum and frequency comb in a nitrobenzene-core photonic crystal fiber with all-normal dispersion profile. Opt. Commun. **481**, 126555 (2021).

Hu, J., Menyuk, C.R., Shaw, L. B., Jasbinder S. Sanghera, Aggarwal, I. D: Maximizing the bandwidth of supercontinuum generation in As_2Se_3 chalcogenide fibers. Optics Express **18**, 6722-6739 (2010).

Hui, Z. Q., Gong, J. M., Liang, M., Zhang, M. Z., Wu, H. M.: Demonstration of all-optical RZ-to-NRZ format conversion based on self-phase modulation in a dispersion flattened highly nonlinear photonic crystal fiber. Opt. Laser Technol. 54, 7-14 (2013).

Hui, Z. Q., Zhang, J.: Design of optical time-division multiplexed systems using the cascaded four-wave mixing in a highly nonlinear photonic crystal fiber for simultaneous time demultiplexing and wavelength multicasting. J. Optics **17**, 075702 (2015).

Hui, Z., Qu, M., Li, X., Guo, Y., Li, J., Jing, L., Wu, Z.: SnS nanosheets for harmonic pulses generation in near infrared region. Nanotechnology **31**, 485706 (2020).

Hui, Z., Xu, W., Li, X., Guo, P., Zhang Y., Liu, J.: Cu_2S nanosheets for ultrashort pulse generation in the near-infrared region. Nanoscale **11**, 6045–6051 (2019).

Kalantari, M., Karimkhani, A., Saghaei. H.: Ultra-wide mid-IR supercontinuum generation in As_2S_3 photonic crystal fiber by rods filling technique. Optik **158**, 142-151(2018).

Karim, M. R., Ahmad, H., Rahman, B. M. A.: All-normal dispersion chalcogenide PCF for ultraflat mid-infrared supercontinuum generation. IEEE Photonics Technol. Lett. **29**, 1792-1795 (2017).

Krishna, G. D., Prasannan, G., Sudheer, S. K., Pillai, V. P. M.: Analysis of zero dispersion shift and supercontinuum generation at near IR in circular photonic crystal fibers. Optik **145**, 599-607 (2017).

Li, J., Zhao, F., Hui, Z.: Mid-infrared supercontinuum generation in dispersion-engineered highly nonlinear chalcogenide photonic crystal fiber. Modern Physics Lett. **B33**, 1950211 (2019).

Maji, P. S., Chaudhuri, P. R.: Design of all-normal dispersion based on multi-material photonic crystal fiber in IR region for broadband supercontinuum generation. Appl. Opt. **54**, 4042-4048 (2015).

Maji, P. S., Chaudhuri, P. R.: Supercontinuum generation in ultra-flat near zero dispersion PCF with selective liquid infiltration. Optik **125**, 5986-5992 (2014).

Medjouri, A., Abed, D., Becer, Z.: Numerical investigation of a broadband coherent supercontinuum generation in $Ga_8Sb_{32}S_{60}$ chalcogenide photonic crystal fiber with all-normal dispersion. Opto-Electronics Rev. **27**, 1-9 (2019).

Medjouri, A., Abed, D.: Design and modelling of all-normal dispersion $As_{39}Se_{61}$ chalcogenide photonic crystal fiber for flat-top coherent mid-infrared supercontinuum generation. Optical Fiber Technol. **50**, 154-164 (2019a).

Medjouri, A., Abed, D.: Mid-infrared broadband ultraflat-top supercontinuum generation in dispersion engineered Ge-Sb-Se chalcogenide photonic crystal fiber. Optical Materials **97**, 109391 (2019b).

Mohebzadeh-Bahabady A., Olyaee, S.: Designing an ultracompact all-optical 4-to-2 encoder and investigating its optical power consumption. Appl. Opt. **59**, 2409-2415 (2020).

Prandin, F.: Realization of ultra-compact all-optical universal NOR gate on photonic crystal platform. J. Electr. Comput. Eng. Innovations **9**, 185-192 (2021).

Romano, C., Jaouën, Y., Tench, R. E., Delavaux, J. M.: Ultra-flat supercontinuum from 1.95 to 2.65 μm in a nanosecond pulsed Thulium-doped fiber laser. Opt.l Fiber Technol. **54**, 102113 (2020).

Russell, P.: Photonic crystal fibers. Science **299**, 358-362 (2003).

Saini, T. S., Kumar, A., Sinha, R. K.: Broadband mid-IR supercontinuum generation in As_2Se_3 based chalcogenide photonic crystal fiber: A new design and analysis. Opt. Commun. **347**, 13-19 (2015).

Saldaña-Díaz, J. E., Jarabo, S., Salgado-Remacha, F. J.: Supercontinuum source based on all-silica fibers with optimized spectral power from 1100 up to 2300 nm. Opt. Laser Technol. **117**, 79-78 (2019).

Seifouri, M., Olyaee, S., Dekamin, M., Karami, R.: Dispersion compensation in optical transmission systems using high negative dispersion chalcogenide/silica hybrid microstructured optical fiber. Optical Rev. **24**, 318-324 (2017a).

Seifouri, M., Olyaee, S., Karami, R.: A new design of As_2Se_3 chalcogenide nanostructured photonic crystal fiber for the purpose of supercontinuum generation. Current Nanoscience **13**, 202-207 (2017b).

Sharma, R., Kaur, S., Chauhan, P., Kumar, A.: Computational design & analysis of $GeSe_2$-As_2Se_3-PbSe based rib waveguide for mid-infrared supercontinuum generation. Optik **220**, 165032 (2020).

Shi, W., Fang, Q., Zhu, X., Norwood, R. A., Peyghambarian, N.: Fiber lasers and their applications. Appl. Opt. **53**, 6554-6568 (2014).

Siwach, P., Kumar, A., Saini, T. S.: Broadband supercontinuum generation spanning 1.5–13 μm in $Ge_{11.5}As_{24}Se_{64.5}$ based chalcogenide glass step index optical fiber. Optik **156**, 564-570 (2018).

Veisi, E., Seifouri, M., **Olyaee**, S.: A novel design of all-optical high speed and ultra-compact photonic crystal AND logic gate based on the Kerr effect, Appl. Physics B. **127**, 1-9 (2021).

Vyas, S., Tanabe, T., Tiwari, M., Singh, G.: Mid-infrared supercontinuum generation in $Ge_{11.5}$ $As_{24}Se_{64.5}$ based chalcogenide photonic crystal fiber. In 2016 Int. Conf. Advances in Computing, Communications and Informatics (ICACCI), pp. 2521-2526. IEEE, 2016.

Wang, Y., Li, S., Chen, H., Shi, M., Liu, Y.: Ultra-wide bandwidth polarization filter based on gold-coated photonic crystal fiber around the wavelength of 1.55 μm. Opt. Laser Technol. **106**, 22-28 (2018).

Xing, S., Kharitonov, S., Hu, J., Brès, C. S.: Linearly chirped mid-infrared supercontinuum in all-normal-dispersion chalcogenide photonic crystal fibers. Optics Express **26**, 19627-19636. (2018).

Yan, P., Dong, R., Zhang, G., Li, H., Ruan, S., Wei, H., Luo, J.: Numerical simulation on the coherent time-critical 2–5 μm supercontinuum generation in an As_2S_3 microstructured optical fiber with all-normal flat-top dispersion profile. Opt. Commun. **293**, 133-138 (2013).

Yuan, W.: 2–10 μm mid-infrared supercontinuum generation in As_2Se_3 photonic crystal fiber. Laser Physics Lett. **10**, 095107 (2013).

Zhang, X., He, M., Chang, M., Chen, H., Chen, N., Qi, N., Yuan, M., Qin, X.: Dual-cladding high-birefringence and high-nonlinearity photonic crystal fiber with As_2S_3 core. Opt. Commun. **410**, 396-402 (2018).

Zhao, L., Li, Y., Guo, C., Zhang, H., Liu, Y., Yang, X., Wang, J., Jing, F., Feng. G.: Generation of 215 W supercontinuum containing visible spectra from 480 nm. Optics Commun. **425**, 118-120 (2018).